

ENSTATITE CHONDRITE OUTGASSING AND CONDENSATE FORMATION: IMPLICATIONS FOR EARLY ATMOSPHERE DEVELOPMENT. B. A. Anzures¹, M. Telus², F. M. McCubbin³, M. A. Thompson⁴, R. Jakubek¹, M. Fries³, J. V. Clark¹. ¹Jacobs, NASA Johnson Space Center. ²Department of Astronomy and Astrophysics, University of California Santa Cruz, ³ARES, NASA Johnson Space Center. ⁴Department of Earth Sciences, ETH-Zürich. Email: brendan.a.anzures@nasa.gov

Introduction: Early atmospheres on rocky planets where life may develop form through outgassing of their original starting blocks, likely a mixture of chondritic material (carbonaceous chondrites (CC), ordinary chondrites (OC), and enstatite chondrites (EC)). However, there is limited experimental data to inform models connecting a planet's bulk composition to its early atmospheric properties and thus its possibility for life. Thompson et al. (2021) [1] took a major step forward in exploring this knowledge gap by measuring outgassing of 3 volatile-rich CCs, providing important experimental constraints on the initial chemical composition of early rocky planet atmospheres. These data provided novel insights into the gas chemistry released into evolving atmospheres early in a rocky planet's history and differed from those currently assumed by many theoretical models of rocky planet atmosphere formation [e.g., 2,3]. In this study, we focused on the outgassing and condensation reactions of a primitive EC3, which has a lower intrinsic oxygen fugacity (f_{O_2}) and lower volatile content than the CCC meteorites investigated by [1]. We selected the EC to explore differences between EC and CC in low-pressure, high-temperature outgassing and condensation including S, Cl, Na, and C species.

Methods: We studied one enstatite chondrite meteorite, an EL3 chondrite Larkman Nunatak (LAR) 12156. The meteorite chip was powdered with 150 mg allocated for the vapor deposition experiment and 10 mg for the outgassing measurement.

Vapor deposition experiments with a temperature gradient from 1200 °C to room temperature (~25 °C) were conducted as evacuated silica tube experiments heated in a 1-bar Deltech furnace at NASA Johnson Space Center (JSC). These experimental conditions match the maximum temperatures of complementary measurements of the outgassing compositions and mass loss using a thermal gravimeter (TG) / differential scanning calorimeter (DSC) / evolved gas analysis (EGA) LABSYS evo instrument at NASA JSC. TG/DSC/EGA measurements were performed with a heating rate of 5 °C/minute at a pressure of 30 mbar of He. The advantage of using an evacuated silica tube is that gases migrate from the hot spot to cooler regions and partially condense to form a thin coating at various temperatures along the tube wall. Importantly, this tells us about species that degas during TG measurements but precipitate in the gas line (typically heated to 100 °C) before reaching the EGA mass spectrometer detectors.

Initial characterization of vapor deposits were

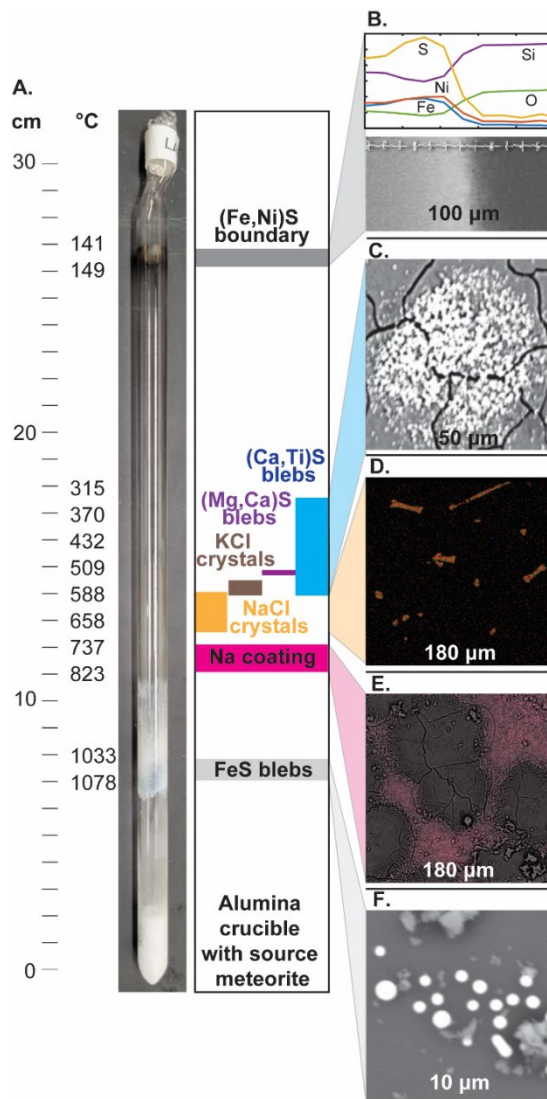


Figure 1. A. Silica tube containing meteorite vapor deposits from EL3 LAR 12156 with temperatures measured using a type B/K thermocouple. B. Sharp (Fe,Ni)S boundary of sulfide coating observed in an EDS image and transect. C. Aggregate (Ca,Ti)S blebs with individual sulfides blebs 1-2 µm in size observed in an EDS image. D. NaCl crystals 5-15 µm in size with lengths up to 50 µm observed in an elemental NaClCa RGB image. E. Interspersed Na coating observed in an EDS image overlain with a Na elemental map (magenta). F. Aggregate FeS blebs with individual sulfide blebs 1-2 µm in size observed in an EDS image.

conducted using a WITec alpha300R Raman microscope (XMB3000-3003) at NASA JSC. This method allowed determination of precipitate species without breaking open the tubes causing exposure to Earth's atmosphere.

After initial characterization, the silica tubes were longitudinally sectioned and mounted onto petrographic slides using carbon tape.

Chemical characterization was completed using the PhenomXL Benchtop Scanning Electron Microscope (SEM) at Lunar and Planetary Institute and the JEOL 7600 SEM at NASA JSC for energy dispersive spectroscopy (EDS) analysis, and the Thermoscientific Apreo FE-SEM at University of California Santa Cruz (UCSC) for elemental mapping and EDS spot analyses. The PhenomXL instrument was operated in low vacuum mode without a carbon coat, while a carbon coat of 20 nm was added for further analysis. To prevent charging, carbon paste was added to the edges of the glass sections before measurements using the Thermofischer Apreo FE-SEM and Oxford Instruments EDS detector (1nA, 15kV)

Condensate Results: SEM EDS analysis and elemental mapping revealed many S and Cl condensates with condensation temperatures marked as the first and last occurrences along the silica tube as shown in Fig. 1. Several S species were identified including FeS blebs (1000-1100 °C), (Ca,Ti)S blebs (300-600 °C), (Ca,Mg)S blebs (~520 °C), and finally a sharp, yet diffuse (Fe,Ni)S film (140-150 °C). Two Cl species were identified as NaCl crystals (600-700 °C) and KCl crystals (550-600 °C). Additionally, a Na-rich coating was observed (700-800 °C).

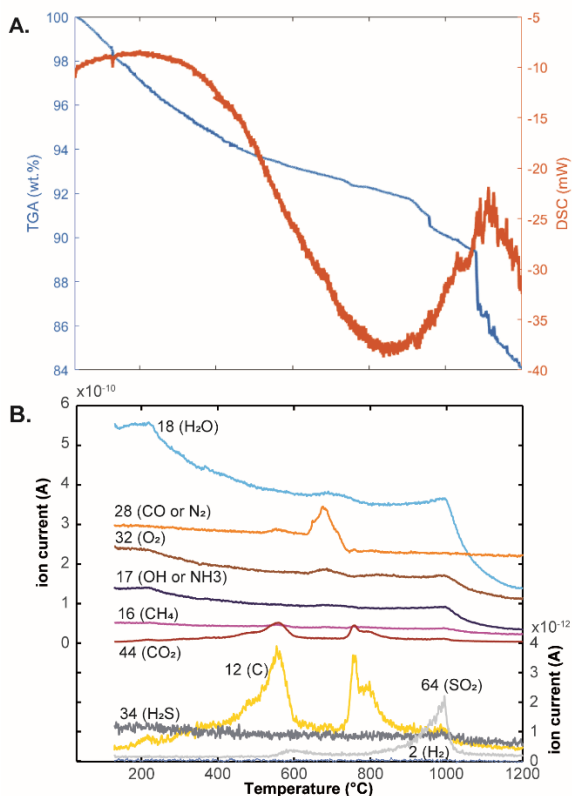


Figure 2. A. TGA (wt.%) weight loss and DSC (heat flow) and B. evolved gas (ion current (A) vs. temperature) for outgassed gases during heating up to 1200 °C.

Our Raman data also indicated macromolecular carbon as numerous 1-2 μm flecks along with a couple thin needles $>100 \mu\text{m}$ in length (300-700 °C). G and D bands were observed at 1361 and 1593 cm^{-1} respectively.

Outgassing Results: TG/DSC/EGA results revealed outgassing of substantial C, S, and H gases as shown in Fig. 2. Carbon gases include C from 400-600 °C and 750-850 °C, CO from 650-750 °C (mass overlap with N₂), and CO₂ from 400-600 °C and 750-850 °C. The only sulfur gas detected was SO₂ being released from 550-650 °C and 850-1000 °C. A small amount of water vapor was detected <250 °C as adsorbed water, and from an unidentified phase at 900-1100 °C. There is also a small O₂ peak at ~ 700 °C.

Implications: Understanding gas-condensed phase interactions aids in reconstructing degassing of planetary magma oceans, planetary atmospheres, evaporation on small planetary bodies, and evaporation during giant impacts [3]. However, a full understanding of evaporation/condensation reactions have classically been limited by poorly constrained oxygen, sulfur, and halogen fugacities [3] especially in reduced, S-rich systems.

Atmospheric and volcanic gases: Experimental results suggest that the atmospheres of reduced and S-rich planetary bodies are composed primarily of CO, CO₂, and SO₂ in contrast with chemical models that suggest N₂ and other C-, Cl-, and S-species [5,6,7], likely due to elements becoming more refractory at reduced conditions. The lack of detectable reduced H-bearing gases including H₂ and H₂S are consistent with Mercury's predicted bone-dry interior [5], although H₂O was detected from an unidentified phase at 900-1100 °C. However, graphitic C, Na metal, Cl salts (NaCl and KCl), and several sulfides were produced during heating and may be important for explosive volcanism, but likely rain down as melts/solids during atmospheric formation.

Exoplanet aerosols: Our experiments provide a link between the composition of outgassing materials, atmospheres, and cloud condensates of rocky planets. Mbarek and Kempton [7] modeled cloud condensate formation for outgassed atmosphere of various chondritic materials. For EL chondrite atmospheres, they found that condensates of K₂SO₄ and ZnO are produced for two super Earth/subNeptune exoplanets. This is inconsistent with our experimental results (Fig. 1) even though the temperature and pressure regimes of our experiments and these models are comparable. Possible reasons could include rainout calculations and/or kinetic effects during outgassing and condensate formation that are not accounted for.

References: [1] Thompson et al. (2021) *Nature Astronomy*, 5, 575-585. [2] Schaefer & Fegley (2010) *Icarus*, 208, 438-448. [3] Sossi & Fegley (2018) *RIMG*, 84, 393-459. [4] Blewett et al. (2011) *Science*, 333, 1856-1859. [5] Zolotov (2011) *Icarus*, 212, 24-41. [6] Deutsch et al. (2021) *EPSL*, 564. [7] Mbarek & Kempton (2016) *Astrophysical Journal*, 827, 121.